Intermetallics 119 (2020) 106721

Contents lists available at ScienceDirect

Intermetallics

journal homepage: http://www.elsevier.com/locate/intermet

Bulk intrinsic heterogeneity of metallic glasses probed by Meissner effect

Shubin Li [a,b], Fujun Lan [b], Songyi Chen [b], Di Peng [b], Yuankan Fang [c], Ren-Shu Wang [b], Hongbo Lou [b], Xin Zhang [b], Zhidan Zeng [b], Xiao-Jia Chen [b], Dong Qian [a,**], Qiaoshi Zeng [b,d,*]

[a] School of Physics and Astronomy, Shanghai Jiao Tong University, Shanghai, 200240, People's Republic of China
[b] Center for High Pressure Science and Technology Advanced Research, Pudong, Shanghai, 201203, People's Republic of China
[c] Department of Physics, University of California, San Diego, La Jolla, CA, 92093, USA
[d] Jiangsu Key Laboratory of Advanced Metallic Materials, School of Materials Science and Engineering, Southeast University, Nanjing, 211189, People's Republic of China

ARTICLE INFO

Keywords:
Metallic glasses
Structural heterogeneity
Atomic structure
Aging
Rejuvenation
Meissner effect
Superconductor

ABSTRACT

Structural heterogeneity has been proposed as a key intrinsic feature and mechanism underline unique properties and dynamic behavior of metallic glasses; however, it is still challenging in precisely describing and effectively characterizing the atomic-scale heterogeneity in metallic glasses. In this work, we employed the Meissner effect of superconductivity in magnetic susceptibility measurements as a sensitive bulk probe and successfully revealed the three-dimensional structural heterogeneity and its two-way evolution tuned by structural aging or rejuvenation in a La-based metallic glass. Compared with the resistivity measurements which only signal the most superconductive loop in inhomogeneous materials, the diamagnetic susceptibility signal of the Meissner effect maps the volumetric distribution of all superconductive regions and the corresponding structural heterogeneity in metallic glasses with high sensitivity. The experimental results reported in this article can be well interpreted based on a structural model of tunable "soft liquid-like" regions with soft vibration modes mixed with "hard solid-like" regions, validating the heterogeneity models of metallic glasses with new experimental data and approach.

1. Introduction

Metallic glasses (MGs) possess many superior properties to both the conventional metals and glasses for widespread applications and also provide unique model systems for fundamental studies of glasses in general [1–5]. Due to the lack of strict restrictions of the well-defined symmetries in crystals and directional bonds in conventional glasses, the atomic structure of MGs has far more degrees of freedom in their atomic arrangement and was expected to be highly disordered and homogeneous before. However, after decades of efforts, it has been gradually recognized that MGs have structural ordering even beyond the nearest-neighbor shell[6,7], and more recently, considerable intrinsic spatial heterogeneity within a certain atomic scale. Especially, the intrinsic spatial heterogeneity is believed to hold the key to understanding many of their unusual properties and behavior in MGs [8–17].

Investigation of the atomic-scale structural heterogeneity in amorphous structures is technically challenging. Recently, some progress using various advanced atomic force microscopy [12,13,18] and scanning transmission electron microscopy [15] has been made to determine the spatial fluctuations of moduli, energy dissipation, or density with correlation lengths of 2.5–20 nm in MGs. These studies are encouraging, however, limited to probing an extremely thin layer or only the surface of MGs and usually involve debatable effects caused by surface oxidation/contamination or high energy electron/iron radiation. Moreover, the surface (nanometer scale) of MGs has been suggested to have different structure/dynamics compared with the interior of MGs [19,20]. However, it is much more challenging to detect the interior of bulk MGs than their surfaces, and it has rarely been done. One major approach to exploring bulk structural heterogeneity studies the anelastic response of MGs to uniaxial mechanical loading. Based on the anisotropic pair distribution function (PDF) analysis of MGs under uniaxial elastic loads, Dmowski et al. [10] reported that MG samples may have ~24% liquid-like atomic packing accounting for their corresponding anelastic deformation [21]. In another high-frequency dynamic

* Corresponding author. Center for High Pressure Science and Technology Advanced Research, Pudong, Shanghai, 201203, People's Republic of China.
** Corresponding author. School of Physics and Astronomy, Shanghai Jiao Tong University, Shanghai, 200240, People's Republic of China
E-mail addresses: dqian@sjtu.edu.cn (D. Qian), zengqs@hpstar.ac.cn (Q. Zeng).

https://doi.org/10.1016/j.intermet.2020.106721
Received 19 December 2019; Received in revised form 23 January 2020; Accepted 24 January 2020
Available online 31 January 2020

micro-pillar compression experiments by Ye et al. [11], ~10% volume fraction of soft liquid-like zones were claimed in MGs according to the significant mechanical hysteresis during uniaxial loading and unloading. In addition, nanoindentation pop-in statistical tests also have been employed to study the structural heterogeneity based on a defect assisted model. The "defect" density can be obtained by fitting, which can be significantly reduced by annealing [22].

According to the previous studies mentioned above, although the details are elusive, structural heterogeneity with two distinct regions (i.e., the relative loosely packed liquid-like soft region and the densely packed solid-like hard region) is believed to exist in MGs. However, besides mechanical properties, structural heterogeneity has been seldom confirmed by other properties measurements. MGs are a class of unique glasses which are electrically conductive; many of them are even superconductors [23]. Superconductivity is a highly structure-sensitive phenomenon (electrons acting as Cooper pairs via electron-phonon interaction), which has been extensively studied in many MG systems, e.g., in the La-based MGs [23–27]. The superconducting behavior of MGs was found to be susceptible to their glass states (structures) as well [28–31]. However, the previous understanding of heterogeneity in MGs mainly referred to the extrinsic structural fluctuation caused by accidently occurred nano-crystallization/precipitation or phase separation, which was not a major topic for superconducting studies of MGs. Based on the current structural model of MGs, heterogeneity is a key feature of the intrinsic structures of MGs, it is naturally expected that the superconducting transition width should be quite broad compared with their single-phase crystalline counterparts. However, surprisingly, the transition width in MGs was found to be as sharp (~a few mK) as single-phase crystalline superconductors[32], which causes confusion and casts doubts on our current structural models of MGs. To address this issue, in this work, we chose a superconductive $La_{75}Al_{25}$ MG as a model system and systematically studied the superconductivity behavior of as-quenched samples together with aged and rejuvenated samples (deliberately tuned structures for structural model validation) using both electronic resistance and magnetic measurements.

2. Experimental details

$La_{75}Al_{25}$ ingots were prepared by melting pure La (99.9 at.%) and Al (99.9 at.%) in an arc-melting machine under a Ti-gettered high purity Ar atmosphere. Each ingot was flipped and melted at least five times to ensure homogeneity in the composition. A melt-spinning device was used to quench the melt droplets into thin ribbons with a copper wheel spinning at 50 m/s. The pure amorphous nature of the as-quenched and annealed MG ribbons was verified by synchrotron radiation x-ray diffraction (XRD), synchrotron radiation small-angle X-ray scattering (SAXS) as shown in Fig. 1, and differential scanning calorimeter (DSC) (Perkin-Elmer 8500), as shown in Fig. 2. The synchrotron radiation XRD measurements were performed at beamline 13-ID-D, Advanced Photon Source (APS), Argonne National Laboratory (ANL), USA. The X-ray wavelength was 0.4959 Å, and the focused beam size was about 2.5 × 3.5 μm^2. The exposure time for each XRD pattern was 60 s. The synchrotron radiation small-angle X-ray scattering (SAXS) was performed at beamline 12-ID-B, APS, ANL to confirm the homogeneity of the MG samples in nanoscale. The X-ray wavelength was 0.9322 Å. The beam size was about 200 × 30 μm^2. In the DSC measurement, the samples were continuously heated at a rate of 20 K/min in the range from 250 K to 723 K, and the cooling rate was 50 K/min under a high-purity nitrogen atmosphere. The electrical and magnetic measurements were carried out by PPMS-9T (Physical Property Measurement System, made by Quantum Design, USA) and MPMS-3 (Magnetic Property Measurement System, made by Quantum Design, USA), respectively. The AC mode was used for resistivity measurements, and the amplitude of current was 100 μA. The standard four-probe method was applied to the flat plane of the ribbon samples. In magnetic measurements, the MG ribbons were cut into several short segments and each segment was

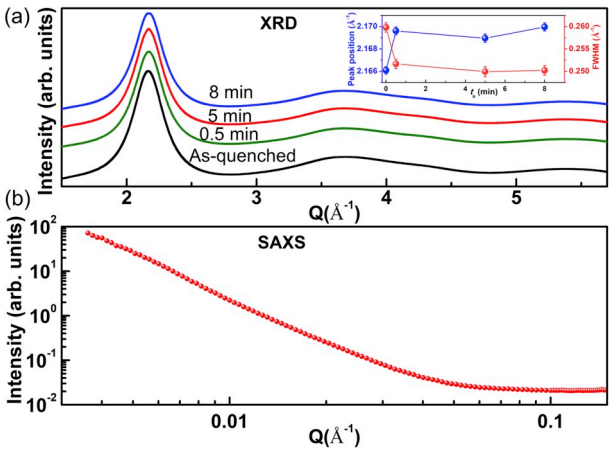

Fig. 1. Structure characterization of $La_{75}Al_{25}$ MG samples by synchrotron radiation x-ray techniques. (a) Synchrotron radiation XRD patterns of the as-quenched and annealed $La_{75}Al_{25}$ MG samples. The inset shows the relative peak position and width changes of the principal peaks. (b) The synchrotron radiation SAXS for the as-quenched $La_{75}Al_{25}$ MG sample.

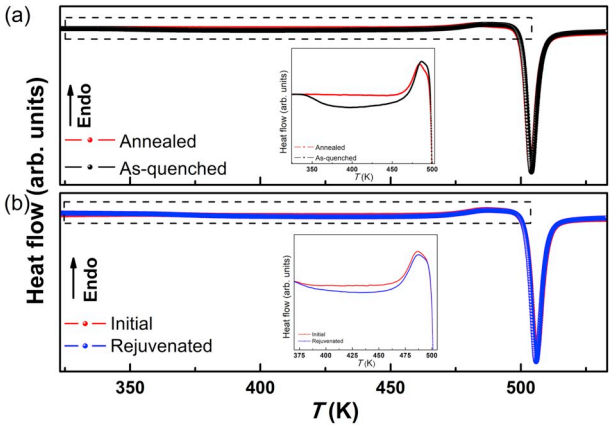

Fig. 2. The DSC characterization of the glass nature and structural relaxation in $La_{75}Al_{25}$ MG samples. (a) The DSC traces for the as-quenched and the annealed (453 K for 5 min) $La_{75}Al_{25}$ MG samples. (b) The DSC traces for the well-relaxed and rejuvenated (27 cycles between 293 K and 77 K) $La_{75}Al_{25}$ MG samples. The insets highlight the comparison of the structural relaxation signals before glass transitions between samples.

attached to the stick for SQUID-VSM measurements to ensure that the magnetic field applied was parallel to the plane of the ribbons. In this way, the effect of the demagnetization factor can be ignored since the sum of the length of the segments was around 30 mm, which is much larger than the width and thickness (the thickness of samples is approximately 20 μm) [33]. Consequently, the variation of diamagnetic susceptibility at 1.8 K reflects the intrinsic properties of the samples rather than the size effect. The DC magnetization for all the samples was measured under a relatively low magnetic field of 20 Oe (below the lower critical field, H_{c1}, at 1.8 K). A low magnetic field of 20 Oe was also applied in the field cooling (FC) process. The reliability of magnetic measurements was also certified by using different sizes of segments to repeat the experiments.

Glass structures were modified by both aging and rejuvenating the $La_{75}Al_{25}$ MGs [34]. Annealing MGs at relatively high temperatures (close to the glass transition temperature, T_g) is an effective way to accelerate the structural aging [35]. The amorphous ribbons were heated in a furnace under a flowing high purity nitrogen atmosphere to conduct the annealing experiments. The annealing samples were heated from room temperature (20 K/min) to 453 K (~21 K below T_g, ~474 K)

and then maintained for 0 min, 0.5 min, 1 min, 5 min, 8 min, and 10 min, respectively, before rapidly cooling down to room temperature. Recently, it was reported that rejuvenation of MGs could be easily realized by thermal cycling between room temperature (293 K) and liquid nitrogen temperature (77 K) [34]. More soft liquid-like regions are expected to be generated in this process at the expense of the hard solid-like matrix. As a result, it is an appropriate method of tuning the local atomic structure but without any destructive effect or shape change for samples as a reverse process of aging for MGs. In this work, thermal cycling treatments were performed by inserting the MG ribbons into a liquid nitrogen Dewar for 1 min and then quickly transferring them into ethanol (constantly maintained at 293 K) for 1 min, then repeating the process for designed cycles.

3. Results and discussion

3.1. Characterization of the amorphous nature

Fig. 1(a) shows the synchrotron radiation XRD patterns of the as-quenched and annealed $La_{75}Al_{25}$ samples. No sharp Bragg diffraction peaks were observed besides the broad, amorphous halos in these patterns. The fitted peak position and peak width of the principal peaks are shown in the inset of Fig. 1(a). The peak position shift caused by annealing is estimated to be ~0.16% and the peak width shrinks by ~3.8% when the annealing time is longer than 0.5 min at 453 K. According to the Debye formula [36], the relative increase of the sample density after annealing is estimated to be ~0.48%. The SAXS experiment performed on the as-quenched $La_{75}Al_{25}$ sample shows smoothly decayed intensity without any bumps as shown in Fig. 1(b), indicating high-quality of the monolithic MG samples without any of the nanoscale density fluctuation. It should be emphasized that the existence of extrinsic heterogeneity caused by a nano-crystalline nucleus or phase separation is explicitly ruled out by the high-resolution synchrotron radiation XRD and SAXS, ensuring the studies in this work could focus on intrinsic amorphous structures of MGs. Moreover, a fully crystallized sample was also obtained as a control sample for comparison by holding the as-quenched $La_{75}Al_{25}$ MG sample above the T_x (the onset temperature of the first peak of crystallization) at 513 K for 5 min. All the samples were also characterized by DSC (Fig. 2). The T_g (glass transition temperatures) and T_x of all the samples including as-prepared, annealed, and rejuvenated samples are nearly identical. In contrast, the enthalpy of relaxation (the exothermal signal before the glass transition) significantly diminished or enhanced are consistent with the effects of annealing or rejuvenation previously reported on MGs, respectively [34].

3.2. Electrical and magnetic properties of as-quenched MG at low temperatures

The zero-field (ZF) electrical resistance of the as-quenched $La_{75}Al_{25}$ sample from 1.8 K to 300 K is shown in Fig. 3(a). Consistent with the prototypical behavior of MGs, the as-quenched $La_{75}Al_{25}$ sample exhibits a negative temperature coefficient of resistance (TCR) above 3.6 K, however, further decrease of the temperature results superconductivity in the sample. Electrical resistance *vs.* temperature at various external magnetic fields up to 3.8 T in the temperature range below 3.7 K is displayed in Fig. 3(b). The superconducting transition temperature T_c from electrical measurements was determined by the 50% criterion. The calculated upper critical field (Fig. 3(c)), $H_{c2}(0)$, at 0 K is ~5.8 T according to the Werthamer-Helfand-Hohenberg (WHH) theory [37] and ~5.7 T based on the theory by Maki [38] and de Gennes [39]. Then, the superconducting coherence length, ξ, can be further calculated to be ~7.6 nm [40] or ~6.5 nm with correction due to short mean free path [41], which are comparable with the proposed characteristic sizes of shear transformation zones (STZs), flow units, or loose packing domains in MGs [18,42,43]. Therefore, these coherence lengths might be

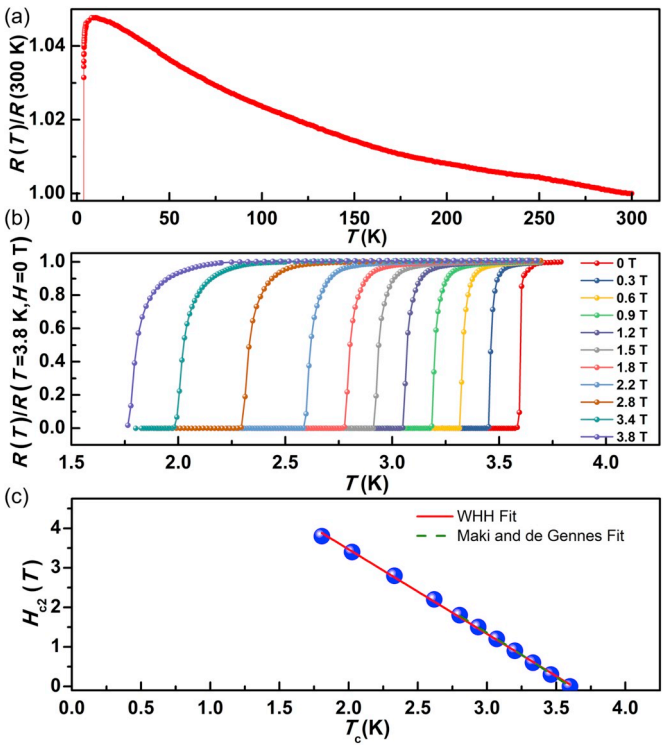

Fig. 3. Electric resistance measurements at low temperatures and various magnetic fields. (a) The resistance as a function of temperature for $La_{75}Al_{25}$ without a magnetic field. The current was 100 μA. (b) The magnetic field dependence of the superconducting transitions in fields from 0 to 3.8 T. (c) The superconducting upper critical field H_{c2} as a function of temperature for $La_{75}Al_{25}$ MGs fitted by a linear correlation to determine the $(dH_{c2}/dT)_{T=Tc}$ used in WHH formula (red curve) and fitted by the formula proposed by Maki and de Gennes (green curve).

associated or interact with the spatial heterogeneity domains in MGs, suggesting close correlation between superconducting behavior and glass structure in MGs. However, the sharp superconducting transitions (<0.02 K) observed in the resistance measurements are comparable to the superconducting transition widths of conventional crystalline metallic superconductors. Given an inhomogeneous superconductor sample, the resistance will be dominated by the most superconductive loop inside the sample and the less conductive regions will be shorted out [44]. As a result, the superconducting transition widths, ΔT_c, in these electronic resistance studies were minimal (around a few mK) and, thus, may not reflect the possible spatial heterogeneity in MGs.

Alternatively, according to the Meissner effect of superconductors (the nature of superconductors to actively exclude magnetic fields from their interiors), a magnetic (diamagnetic susceptibility) measurement could catch more bulk information on the superconductivity of the entire sample with heterogeneity. The temperature dependence of the magnetic susceptibility of the $La_{75}Al_{25}$ MG sample was, therefore, further characterized, as shown in Fig. 4(a). The difference between zero-field cooling (ZFC) data and FC data is ascribed to the flux pinning in type-II superconductor [45]. If we define the temperature at which the sample starts to show a signal of diamagnetic susceptibility as the onset T_c, the as-quenched $La_{75}Al_{25}$ MG sample possesses a striking diamagnetic superconducting transition at ~3.6 K, which is consistent with the value of T_c estimated by resistance measurement in Fig. 3(a). However, the transition width observed in the diamagnetic susceptibility measurement is much broader than that in the resistance measurement. For comparison, the magnetization of the crystallized sample was also measured, as shown in Fig. 4(b). Only one superconducting transition was observed at a higher transition temperature, ~4.3 K, and the transition width is sharp as expected for crystals. Based on the

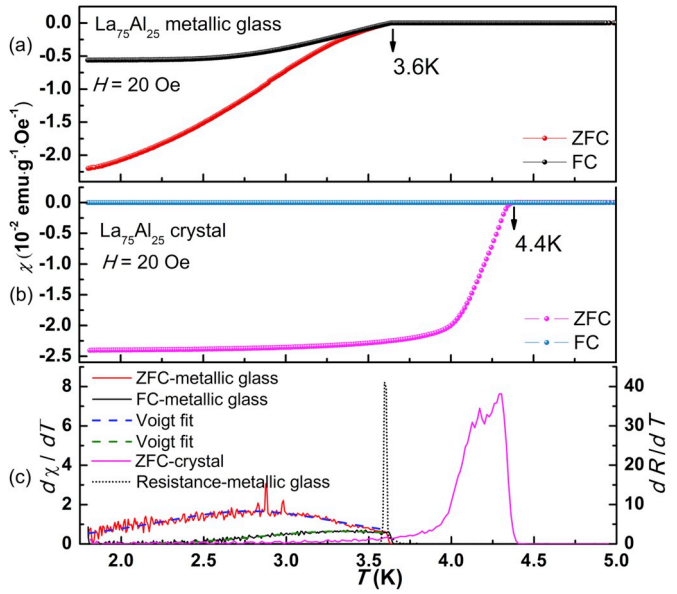

Fig. 4. Magnetic susceptibility measurements through the superconducting transitions of the $La_{75}Al_{25}$ samples. Temperature dependence of magnetic susceptibility with FC or ZFC from 1.8 K to 5 K for the as-quenched $La_{75}Al_{25}$ MG, (a) and the crystallized $La_{75}Al_{25}$ sample (b). The applied magnetic field was 20 Oe. (c) The derivative of the diamagnetic susceptibility data in (a) and (b) compared with the derivative of the resistance data (dotted line) in Fig. 3(a) as a function of temperature.

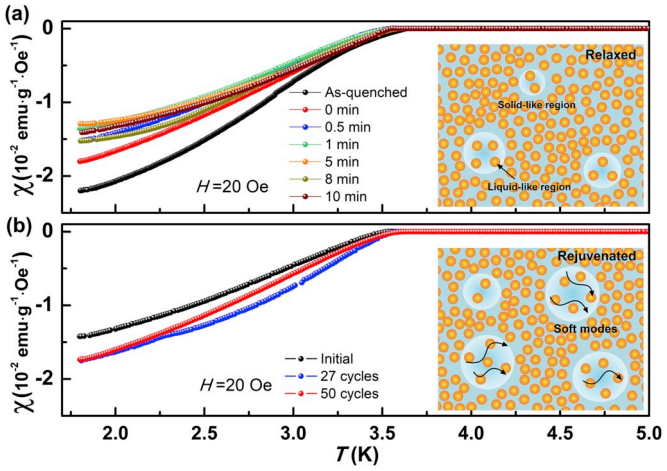

Fig. 5. Magnetic susceptibility measurements through the superconducting transitions of the $La_{75}Al_{25}$ samples after aging or rejuvenation treatment. Temperature dependence of magnetic susceptibility with FC or ZFC from 1.8 K to 5 K for as-quenched $La_{75}Al_{25}$ and annealed MG samples (a) and for the initial sample $La_{75}Al_{25}$ (well-relaxed) and the rejuvenated samples by thermally cycling 27 and 50 times (b). The insets in (a) and (b) present the schematic illustration for the atomic structure of MGs tuned by aging and rejuvenation, respectively. It should be noted that the liquid-like regions and solid like regions in real structures of MGs may not have definable boundaries between them as simplified in these illustrations.

analysis of the XRD patterns of the fully crystallized $La_{75}Al_{25}$ sample, the single superconducting phase should be the crystallized α-La [46]. The transition widths can be readily estimated by the peak widths of the derivative curves of the diamagnetic susceptibility data (Fig. 4(c)). The transition width of the $La_{75}Al_{25}$ MG sample is approximately 6 times larger than that of the crystallized sample. As the superconducting transition width is supposed to be related to the heterogeneous structure in superconductors[47–49], the superconducting phase in the $La_{75}Al_{25}$ MG is obviously much more heterogeneous than that in its crystallized products. Moreover, the superconducting transition shown in the ZFC curve of the $La_{75}Al_{25}$ MG is broad but quite smooth without obvious steps, indicating that the heterogeneity in MGs may have a continuous and wide statistical distribution rather than consisting of two-distinct domains (as typically simplified as liquid-like and solid-like regions). This speculation is further supported by the broad peaks in the derivative of the diamagnetic susceptibility data for both ZFC and FC measurements in MG samples (Fig. 4(c)), which indicates a wide distribution of the superconducting transition temperatures as well.

3.3. The nominal shielding volume fraction for annealing and thermal cycling

To further clarify and validate the close correlation between diamagnetic susceptibility and glass structure/states, structural tuning was achieved deliberately in a two-way manner by thermal treatment of aging and rejuvenation [34]. Fig. 5 shows the temperature dependence of magnetic susceptibility from 1.8 K to 5 K for $La_{75}Al_{25}$ MG samples with different annealing time or rejuvenation thermal cycles. From the ZFC data, the magnitude of diamagnetic susceptibility for per unit mass of the $La_{75}Al_{25}$ MG under a magnetic field of 20 Oe at 1.8 K is defined as the nominal shielding volume fraction (although no plateau is reached). With the increase of annealing time or thermal cycles, both the T_c (Fig. 6 (a) and (c)) and the nominal shielding volume fraction (Fig. 6(b) and (d)) could be dramatically and consistently deduced and increased, respectively. However, the changes of T_c are much smaller than that of the nominal shielding volume fraction (e.g., ~2.5% vs. ~38% with the annealing time of 1 min at 453 K). These results further demonstrate that the shielding volume fraction is a more sensitive and capable variable compared with the "conventional" shift of T_c to characterize the structural states/evolution in MGs.

3.4. The mechanism based on the core-shell model and the theory of soft phonon modes

The superconducting MGs are believed to be weak or mediate phonon-electron coupling type-superconductors under dirty limit and could be described in the frame of conventional BCS theory [28], in which the superconductivity is strongly associated with the electron-phonon coupling constant, λ. Poon [29] and Inoue [50] both mentioned that the annihilation of quench-in 'defects' or the 'hardening' of the phonon modes is responsible for the degradation in λ, therefore, in T_c for structural relaxation in their studies on MGs. Ding et al. [14] and Zhang et al. [51] have reported that liquid-like regions in MGs possess a high propensity to stimulate soft modes. As a result, during annealing, the degradation of liquid-like soft regions in MGs causes the reduction of the quasi-local soft modes (the inset of Fig. 5(a)), consequently, diminishing of λ, nominal shielding volume, and T_c. On the other hand, more soft spots or liquid-like regions generated by the rejuvenation process would result in a rising number of soft modes (the inset of Fig. 5(b)), therefore, increasing nominal shielding volume and T_c with elevated λ. It has been extensively proposed that both the aging and rejuvenation in MGs might be associated with the evolution of structural heterogeneity in atomic scale, i.e., the volume ratio of the solid-like matrix and quench-in liquid-like "defects" regions that make up the MGs could change during structural aging or rejuvenation processes [18,52,53]. The results in this work support this intrinsic structural heterogeneity model of MGs and its mechanism for tuning by aging or rejuvenation.

In addition to the values of the nominal shielding volume fraction and T_c, the entire profile of the ZFC and FC diamagnetic susceptibility curves of MGs also show abnormal behavior compared with that in typical crystalline superconductors. These may provide even more detailed information about the glass structure/states and its distribution and variation tuned by various treatment, e.g., the diamagnetic signal in FC curve of MGs is still prominent compared to their crystallized

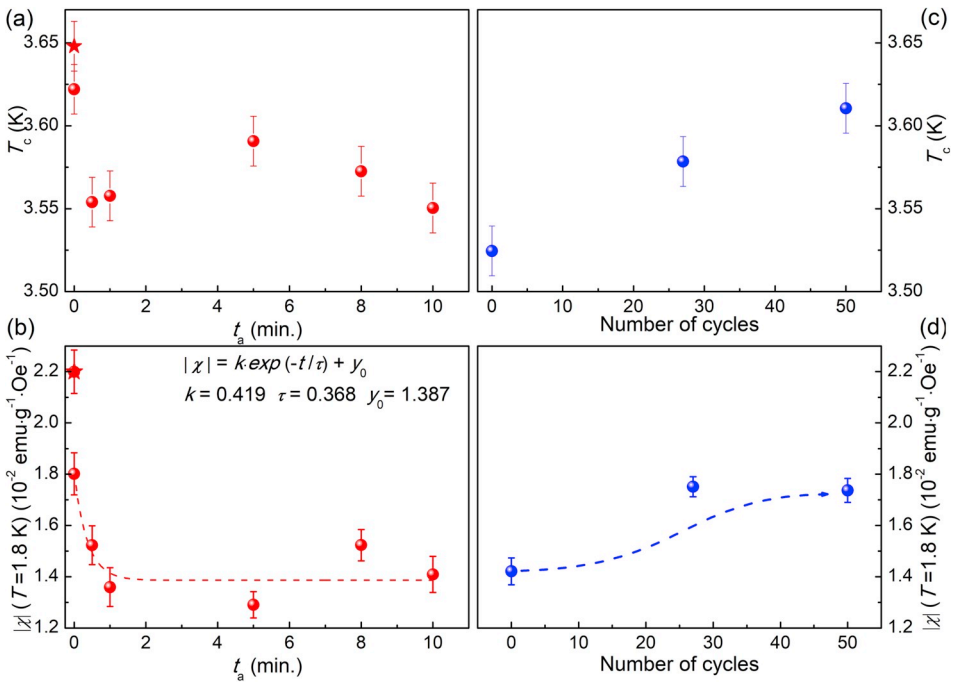

Fig. 6. Onset superconducting temperatures, T_c and absolute nominal shielding volume fractions, $|\chi|$ as a function of the structures tuned by aging or rejuvenation. Holding time for annealing (t_a) dependent T_c (a) and $|\chi|$ (T = 1.8 K) (b) obtained from curves in Fig. 5a. The red pentagrams represent the as-quenched sample. Thermal cycling times dependent T_c. (c) and $|\chi|$ (T = 1.8 K) (d) obtained from Fig. 5b. The red dashed line is a fit following the exponential equation: $|\chi| = k \cdot \exp(-t/\tau) + y_0$, where k is the coefficient, τ is the characteristic relaxation time, y_0 is the offset constant. The blue dashed line is a guide for the eyes.

products due to the MG's relative weak pinning abilities (Fig. 4). However, the superconducting transition shown in FC is much narrower (the curve shape changes) than that in ZFC of MGs. These results suggest that the flux pinning in the MG sample is not uniform, which may be mainly carried by more solid-like (also more ordered and denser) regions with stronger pinning abilities but weaker electron-phonon interaction. Therefore, the remaining superconducting regions presented in the FC measurement might be the most liquid-like regions with softer modes, whose volume fraction can be estimated to be ~25% by the nominal shielding volume fraction ratio between FC and ZFC. Therefore, it is worth further studying to dig deeper and provide more valuable information as constraints on our current glass structure modelling or inspire new models.

4. Conclusions

In summary, we synthesized a model MG sample $La_{75}Al_{25}$ and carefully characterized their structures by synchrotron radiation XRD and SAXS, which rule out the typical extrinsic heterogeneity caused by nano-crystallization or phase separation. Then, we systematically studied the superconducting behavior of the $La_{75}Al_{25}$ MG by magnetic susceptibility measurements and electrical resistance measurements at low temperatures. Compared with the resistance measurements which signal the most conductive one-dimensional loop, the diamagnetic susceptibility is found to be an extremely sensitive bulk probe which can conclusively reveal the three-dimensional spatial structure heterogeneity associated with a broad distribution of T_c in the entire sample. The different structural states of the $La_{75}Al_{25}$ MG sample tuned by relaxation and thermal cycling cause a significant change in the nominal shielding volume fractions which can also be well explained by the structural heterogeneity with the volume fraction change/degradation of the liquid-like regions caused by aging or rejuvenation. Therefore, our findings provide valuable experimental data and systematic explanations to validate and deepen our current understanding of the glass structure and its evolution in MGs. The transition width and ZFC/FC curve shapes from magnetic susceptibility measurements could provide more detailed information about the glass structure and structural tuning by either relaxation or rejuvenation, which are worth further exploration in the future to dig deeper and obtain more valuable experimental data as constraints on our current glass structure modelling or inspire new models.

Declaration of competing interest

The authors declare that they have no known competing financial interests or personal relationships that could have appeared to influence the work reported in this paper.

CRediT authorship contribution statement

Shubin Li: Methodology, Validation, Formal analysis, Investigation, Visualization, Writing - original draft. **Fujun Lan:** Methodology, Validation, Formal analysis, Investigation, Visualization. **Songyi Chen:** Investigation. **Di Peng:** Investigation. **Yuankan Fang:** Investigation, Writing - review & editing. **Ren-Shu Wang:** Investigation. **Hongbo Lou:** Investigation. **Xin Zhang:** Investigation. **Zhidan Zeng:** Investigation, Writing - review & editing. **Xiao-Jia Chen:** Methodology, Resources. **Dong Qian:** Methodology, Resources, Formal analysis, Supervision. **Qiaoshi Zeng:** Conceptualization, Methodology, Formal analysis, Writing - review & editing, Supervision.

Acknowledgments

This work was supported by the National Natural Science Foundation of China (Grant No. 51871054, U1930401) and the Fundamental Research Funds for the Central Universities. This research used the beamline 13-ID-D and 12-ID-B at APS. The usage of the beamline 13-ID-D (GeoSoilEnviroCARS) at APS was supported by the National Science Foundation (NSF)-Earth Sciences (EAR-1634415) and Department of Energy (DOE)-GeoSciences (DE-FG02-94ER14466). APS is supported by the DOE, Office of Science, Office of Basic Energy Sciences, under Contract No. DE-AC02-06CH11357. Part of this work used the beamline15U1 of SSRF, China.

Appendix A. Supplementary data

Supplementary data to this article can be found online at https://doi.org/10.1016/j.intermet.2020.106721.

References

[1] W.L. Johnson, Bulk glass-Forming metallic alloys: science and technology, MRS Bull. 24 (10) (1999) 42–56.
[2] C.A. Angell, Formation of glasses from liquids and biopolymers, Science 267 (5206) (1995) 1924–1935.
[3] W.H. Wang, Bulk metallic glasses with functional physical properties, Adv. Mater. 21 (45) (2009) 4524–4544.
[4] M. Chen, A brief overview of bulk metallic glasses, NPG Asia Mater. 3 (9) (2011) 82–90.
[5] J. Schroers, Bulk metallic glasses, Phys. Today 66 (2) (2013) 32–37.
[6] H.W. Sheng, W.K. Luo, F.M. Alamgir, J.M. Bai, E. Ma, Atomic packing and short-to-medium-range order in metallic glasses, Nature 439 (7075) (2006) 419–425.
[7] Q.S. Zeng, H.W. Sheng, Y. Ding, L. Wang, W.G. Yang, J.Z. Jiang, W.L. Mao, H. K. Mao, Long-range topological order in metallic glass, Science 332 (6036) (2011) 1404–1406.
[8] T. Ichitsubo, E. Matsubara, T. Yamamoto, H.S. Chen, N. Nishiyama, J. Saida, K. Anazawa, Microstructure of fragile metallic glasses inferred from ultrasound-accelerated crystallization in Pd-based metallic glasses, Phys. Rev. Lett. 95 (24) (2005), 245501.
[9] T. Fujita, K. Konno, W. Zhang, V. Kumar, M. Matsuura, A. Inoue, T. Sakurai, M. W. Chen, Atomic-scale heterogeneity of a multicomponent bulk metallic glass with excellent glass forming ability, Phys. Rev. Lett. 103 (7) (2009), 075502.
[10] W. Dmowski, T. Iwashita, C.P. Chuang, J. Almer, T. Egami, Elastic heterogeneity in metallic glasses, Phys. Rev. Lett. 105 (20) (2010), 205502.
[11] J.C. Ye, J. Lu, C.T. Liu, Q. Wang, Y. Yang, Atomistic free-volume zones and inelastic deformation of metallic glasses, Nat. Mater. 9 (8) (2010) 619–623.
[12] Y.H. Liu, D. Wang, K. Nakajima, W. Zhang, A. Hirata, T. Nishi, A. Inoue, M. W. Chen, Characterization of nanoscale mechanical heterogeneity in a metallic glass by dynamic force microscopy, Phys. Rev. Lett. 106 (12) (2011), 125504.
[13] H. Wagner, D. Bedorf, S. Küchemann, M. Schwabe, B. Zhang, W. Arnold, K. Samwer, Local elastic properties of a metallic glass, Nat. Mater. 10 (6) (2011) 439–442.
[14] J. Ding, S. Patinet, M.L. Falk, Y. Cheng, E. Ma, Soft spots and their structural signature in a metallic glass, Proc. Natl. Acad. Sci. U.S.A. 111 (39) (2014) 14052–14056.
[15] F. Zhu, A. Hirata, P. Liu, S. Song, Y. Tian, J. Han, T. Fujita, M. Chen, Correlation between local structure order and spatial heterogeneity in a metallic glass, Phys. Rev. Lett. 119 (21) (2017), 215501.
[16] F. Zhu, S. Song, K.M. Reddy, A. Hirata, M. Chen, Spatial heterogeneity as the structure feature for structure-property relationship of metallic glasses, Nat. Commun. 9 (1) (2018) 3965.
[17] J.C. Qiao, Q. Wang, J.M. Pelletier, H. Kato, R. Casalini, D. Crespo, E. Pineda, Y. Yao, Y. Yang, Structural heterogeneities and mechanical behavior of amorphous alloys, Prog. Mater. Sci. 104 (2019) 250–329.
[18] Y. Yang, J.F. Zeng, A. Volland, J.J. Blandin, S. Gravier, C.T. Liu, Fractal growth of the dense-packing phase in annealed metallic glass imaged by high-resolution atomic force microscopy, Acta Mater. 60 (13–14) (2012) 5260–5272.
[19] C.R. Cao, K.Q. Huang, J.A. Shi, D.N. Zheng, W.H. Wang, L. Gu, H.Y. Bai, Liquid-like behaviours of metallic glassy nanoparticles at room temperature, Nat. Commun. 10 (1) (2019) 1966.
[20] L. Chen, C.R. Cao, J.A. Shi, Z. Lu, Y.T. Sun, P. Luo, L. Gu, H.Y. Bai, M.X. Pan, W. H. Wang, Fast surface dynamics of metallic glass enable superlatticelike nanostructure growth, Phys. Rev. Lett. 118 (1) (2017), 016101.
[21] T. Egami, S.J. Poon, Z. Zhang, V. Keppens, Glass transition in metallic glasses: a microscopic model of topological fluctuations in the bonding network, Phys. Rev. B 76 (2) (2007), 024203.
[22] Y. Gao, H. Bei, Strength statistics of single crystals and metallic glasses under small stressed volumes, Prog. Mater. Sci. 82 (2016) 118–150.
[23] W.L. Johnson, Superconductivity and electronic properties of amorphous transition metal alloys, J. Appl. Phys. 50 (B3) (1979) 1557–1563.
[24] W.L. Johnson, S.J. Poon, P. Duwez, Amorphous superconducting lanthanum-gold alloys obtained by liquid quenching, Phys. Rev. B 11 (1) (1975) 150–154.
[25] R. Delgado, H. Armbruster, D.G. Naugle, C.L. Tsai, W.L. Johnson, A. Williams, Electron transport in La100-xAlx metallic glasses, Phys. Rev. B 34 (12) (1986) 8288–8295.
[26] K. Agyeman, R. Müller, C.C. Tsuei, Alloying effect on superconductivity in amorphous lanthanum-based alloys, Phys. Rev. B 19 (1) (1979) 193–198.
[27] M.B. Tang, H.Y. Bai, M.X. Pan, D.Q. Zhao, W.H. Wang, Bulk metallic superconductive La60Cu20Ni10Al10 glass, J. Non-Cryst. Solids 351 (30–32) (2005) 2572–2575.
[28] Z. Altounian, J.O. Strom-Olsen, Superconductivity and spin fluctuations inM−Zr metallic glasses (M=Cu,Ni,Co,and Fe), Phys. Rev. B 27 (7) (1983) 4149–4156.
[29] S.J. Poon, Thermal-relaxation studies of the stability of amorphous structures in zirconium-based superconducting alloys, Phys. Rev. B 27 (9) (1983) 5519–5525.
[30] M. Tenhover, W.L. Johnson, Superconductivity and the electronic structure of Zr- and Hf-based metallic glasses, Phys. Rev. B 27 (3) (1983) 1610–1618.
[31] B. Huang, H.Y. Bai, P. Wen, D.W. Ding, D.Q. Zhao, M.X. Pan, W.H. Wang, The heterogeneous structure of metallic glasses revealed by superconducting transitions, J. Appl. Phys. 114 (11) (2013).
[32] F.E. Luborsky, Amorphous Metallic Alloys, Butterworths, London, 1983.
[33] R. Prozorov, V.G. Kogan, Effective demagnetizing factors of diamagnetic samples of various shapes, Phys. Rev. Appl. 10 (1) (2018), 014030.
[34] S.V. Ketov, Y.H. Sun, S. Nachum, Z. Lu, A. Checchi, A.R. Beraldin, H.Y. Bai, W. H. Wang, D.V. Louzguine-Luzgin, M.A. Carpenter, A.L. Greer, Rejuvenation of metallic glasses by non-affine thermal strain, Nature 524 (7564) (2015) 200–203.
[35] W.H. Wang, Dynamic relaxations and relaxation-property relationships in metallic glasses, Prog. Mater. Sci. 106 (2019), 100561.
[36] A. Guinier, X-ray Diffraction in Crystals, Imperfect Crystals and Amorphous Bodies, W.H. Freeman, San Francisco, 1963.
[37] N.R. Werthamer, E. Helfand, P.C. Hohenberg, Temperature and purity dependence of the superconducting critical field, H_{c2}. III. Electron spin and spin-orbit effects, Phys. Rev. 147 (1) (1966) 295–302.
[38] K. Maki, The magnetic properties of superconducting alloys. II, Physics Physique Fizika 1 (2) (1964) 127–143.
[39] P.G. de Gennes, Behavior of dirty superconductors in high magnetic fields, Phys. Konden. Mater. 3 (2) (1964) 79–90.
[40] M. Tinkham, Introduction to Superconductivity, second ed., McGraw-Hill, Singapore, 1996.
[41] L.P. Gor'kov, Sov. Phys. JETP 10 (1960) 998.
[42] D. Pan, A. Inoue, T. Sakurai, M.W. Chen, Experimental characterization of shear transformation zones for plastic flow of bulk metallic glasses, Proc. Natl. Acad. Sci. U.S.A. 105 (39) (2008) 14769.
[43] S.T. Liu, Z. Wang, H.L. Peng, H.B. Yu, W.H. Wang, The activation energy and volume of flow units of metallic glasses, Scripta Mater. 67 (1) (2012) 9–12.
[44] A. Schilling, M. Cantoni, J.D. Guo, H.R. Ott, Superconductivity above 130 K in the Hg–Ba–Ca–Cu–O system, Nature 363 (6424) (1993) 56–58.
[45] D. Dew-Hughes, Flux pinning mechanisms in type II superconductors, Philos. Mag. A 30 (2) (1974) 293–305.
[46] T.F. Smith, H.L. Luo, Superconductivity of lanthanum and lanthanum compounds at zero and high pressure, J. Phys. Chem. Solid. 28 (4) (1967) 569–576.
[47] S. Lee, T. Masui, A. Yamamoto, H. Uchiyama, S. Tajima, Crystal growth of C-doped MgB2 superconductors: accidental doping and inhomogeneity, Physica C 412–414 (2004) 31–35.
[48] G.E. Zwicknagl, J.W. Wilkins, Measured width of superconducting transition: quantitative probe of macroscopic inhomogeneities, Phys. Rev. Lett. 53 (13) (1984) 1276–1279.
[49] A. Nordström, U. Dahlborg, Ö. Rapp, Variation of disorder in superconducting glassy metals, Phys. Rev. B 48 (17) (1993) 12866–12873.
[50] A. Inoue, K. Matsuzaki, N. Toyota, H.S. Chen, T. Masumoto, T. Fukase, Correlation between structural relaxation enthalpy and superconducting properties of amorphous Zr70Cu30 and Zr70Ni30 alloys, J. Mater. Sci. 20 (7) (1985) 2323–2334.
[51] Y. Zhang, C.Z. Wang, F. Zhang, M.I. Mendelev, M.J. Kramer, K.M. Ho, Strong correlations of dynamical and structural heterogeneities with localized soft modes in a Cu-Zr metallic glass, Appl. Phys. Lett. 105 (15) (2014), 151910.
[52] L.Z. Zhao, Y.Z. Li, R.J. Xue, W.H. Wang, H.Y. Bai, Evolution of structural and dynamic heterogeneities during elastic to plastic transition in metallic glass, J. Appl. Phys. 118 (15) (2015), 154904.
[53] W. Guo, R. Yamada, J. Saida, Rejuvenation and plasticization of metallic glass by deep cryogenic cycling treatment, Intermetallics 93 (2018) 141–147.